Journal of the European Ceramic Society **18** (1998) 81–85

PII: S0955-2219(97)00095-2
0955-2219/98/$19.00 + 0.00

Anisotropic Mechanical Properties in Sinter-Forged Bulk Highly Textured (Bi,Pb)-2223 Ceramics

V. Rouessac[a,b] and M. Gomina[a]

[a] ISMRA/LERMAT, CNRS UPRES-A 6004, 6 Bd Maréchal Juin, F-14050 Caen Cedex, France
[b] ISMRA/CRISMAT, CNRS UMR 6508, 6 Bd Maréchal Juin, F-14050 Caen Cedex, France

(Received 28 January 1997; accepted 17 March 1997)

Abstract

Bi(Pb)SCCO-2223 oxide has been synthesised and then densified into bulk-textured ceramics by the sinter-forging method. Vickers and Knoop indentations and 3-point bending tests have been carried out on specimens to investigate the mechanical anisotropy due to the coarse microstructure and morphological anisotropy of the sinter-forged samples. Our observations showed that the parameters which represent the mechanical properties (H_K, σ_R, K_{IC}), are strongly dependent on the sinter-forging treatment and are mainly affected by both stress level and its application time. © *1997 Elsevier Science Limited.*

1 Introduction

Since the discovery of the Bi-Sr-Ca-Cu-O system, the possibility of obtaining dense bulk and textured bismuth superconductor ceramics by sinter-forging was pointed out. Nevertheless, the mechanical properties of such bulk (Bi,Pb)SrCaCuO ceramics have been partially neglected because attention was mainly focused on the best superconductive properties (higher critical temperature, critical current density, etc.). A few mechanical characterisation studies have been published, focused on 2212 textured ceramics,[1–4], 2223/Ag tapes,[5–7] bulk untextured Ag-Bi2223 composite ceramics[8,9] and bulk monolithic textured Bi-2223 ceramics.[10] The present work deals with $Bi_{1.85}Pb_{0.35}Sr_2Ca_2Cu_{3.1}O_{10+x}$ bulk and textured samples, free of Bi-2212 phase according to X-ray diffraction patterns analysis (XRD) and in which other secondary phases (very weak in XRD) represent a total amount around 5 vol. % in image analysis (Sr-Ca-Cu-O phases). We try to correlate the mechanical properties with the different parameters of the sinter-forging process i.e. stress and time under load (which determine the final deformation and the quality of the final textured bulk ceramic), and with the post-annealing treatment, necessary to recover good superconductive properties. Samples were tested in Vickers and Knoop hardness. Toughness measurements were implemented in the flat-wise orientation of textured samples. The results have been compared with regard to the texture quality. SEM (Philips FEG XL30) was used to analyse the influence of texture on the crack propagation mode and for fractographic observation.

2 Experimental Procedure

The specimens used in the present study were made by sinter-forging at 845°C under 5–20 MPa for several hours[11] a (Bi,Pb)-2223 powder synthesised by a sol–gel method.[12] The 2223 grains of the powder are typically 10 μm wide and 0·2–0·5 μm thick. As-forged samples were 0·5–2 mm thick and 25–50 mm in diameter discs, depending on the sinter-forging time and load. The discs were cut into bars whose sections were diamond-polished. The $(Bi_{1.85}Pb_{0.35})Sr_2Ca_2Cu_{3.1}O_y$ grain boundaries were chemically revealed. We were able thus to observe the texture with the c-axis of the grains more or less parallel to the sinter-forging direction, and the residual secondary phases.

Different specimens were elaborated. The first one (A), with randomly oriented grains, was obtained by cold isostatic pressing and then sintering at 845°C. The other ones were textured after different sinter-forging treatments at 845°C : a coarse-textured sample (B) obtained under 5 min/7 MPa, a better (but too fast) textured sample (C) obtained under 5 min/20 MPa, and two longer sinter-forged specimens under 24 h/15 MPa (D) and

48 h/15 MPa (E). Figure 1 represents the load and equivalent stress profiles as a function of time for the four different sinter-forging conditions. The two long-loading profiles start with a slow increasing of the load to prevent any decomposition of the 2223 oxide of low stability near its fusion temperature. Then the slow creeping of the 2223 platelets implies the deformation and diameter increase that lowers the stress. In terms of texture quality, (0 0 14) pole figures (Philips X'Pert) reveal that 50% of the volume fraction of grains are oriented with the *c*-axis within 14° in specimen (B) and 8° in specimens (D) and (E) (Fig. 2).

The densities of these sinter-forged specimens are nearly the same, around 95% or above of the theoretical one (~6·2 $g\,cm^{-3}$), whereas the density of specimen (A) is only 79%, due to the cold isostatic pressing process (300 MPa) followed by a sintering, that is known to adversely affect densification of the 2223 phase.[13] To compare with a theoretical randomly oriented grains specimen, three isostatic-pressed specimens at 100, 200 and 300 MPa were synthesised to check the relationship between hardness and density. The Knoop hardness of the randomly oriented body (95% dense) was evaluated by extrapolation of the values associated to the three specimens mentioned above (Fig. 3).

A course of Vickers indentation tests at room temperature were carried out on the polished and chemically revealed sections, with a diagonal parallel to the texture orientation. The spectacular influence of the texture on the shape of the Vickers impress after unloading, already observed by the Luo *et al.* study[10] but in less proportion, led to further investigations using Knoop indentation as a function of the disorientation angle α of the impress to the sinter-forging stress axis (Fig. 4).

Fracture toughness measurements were performed using SENB specimens (3-point bending loading) cut from the hot-forged batches (B) to (E). The final thickness of well-textured (C) to (E) pellets are less than 1 mm, which is too small to obtain meaningful results, especially for notched bars cracking. To obtain thicker bars, two or three identical pellets were hot-forged and then pasted together during another short-time sinter-forging treatment. SEM observations on polished cross-sections revealed a complete disappearance of the boundary between the two pellets, even after only two hour long hot-forging. In that way, the final thickness of the pellets (C) to (E) is identical (2 mm) for each texture quality. As-forged, annealed notched bars and smooth ones were tested to assess the flexural strength σ_R, the elastic modulus E and the fracture toughness K_{IC}.

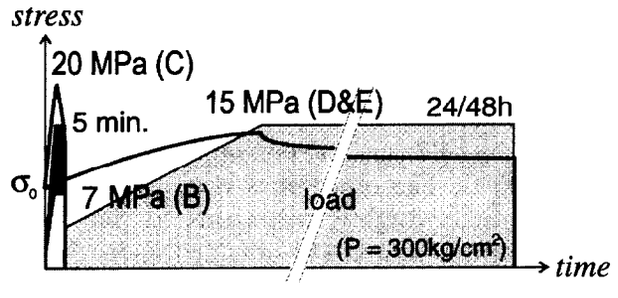

Fig. 1. Different loading profiles adopted in the study as a function of time with the corresponding different stress applied on the (Bi,Pb)-2223 disc (B) to (E).

3 Results and Discussion

3.1 Knoop hardness

When a diagonal of the Vickers impress is parallel to the sinter-forging stress axis, the shape which was squared under the diamond, it transforms into a lozenge when unloading (Fig. 5). The more textured the ceramic, the further the more diagonal ratio is from 1. Those different elastic recoveries in the impress parallel and perpendicular to the sinter-forging axis have been already shown by Luo but with a smaller ratio. No crack but an important decohesion of the grains was observed in (C) direction, around the corners of the impress, since the load was below 50 N. The chemical attack of the polished cross-section reveals agglomerates of grains around 50–100 μm wide, not each 2223 plate-like grain, about 10–20 μm in size. Thus, the indent size is considerably larger than the grain one. The inference is that the anisotropy is due to the macrostructure produced by the orientation of a group of individual grains, rather than due to the effect of crystallographic anisotropy. Table 1 summarises the results of Knoop hardness tests. On the basis of these results, several points may be considered:

(1) For a given sinter-forging time (5 min. samples (B) and (C)) a higher stress induces a higher mean hardness value and a strong difference in the extreme hardness values between 0° to 90° from the sinter-forging axis. It corresponds to a better alignment of the 2223 grains. There is no difference according to the mean size of the grains but the best alignment induces more contacts between grains, thus the best links are along the (*a*,*b*) plane, enhanced by high stress.

(2) For a given load (600 kg, corresponding to a 15 MPa maximal stress) even when the textured aspect is similar according to X-ray pole figure, the hardness along the stress axis is higher for the 48 h sinter-forged sample (E) than in the 24 h one (D). The principal microstructural difference is the final grain

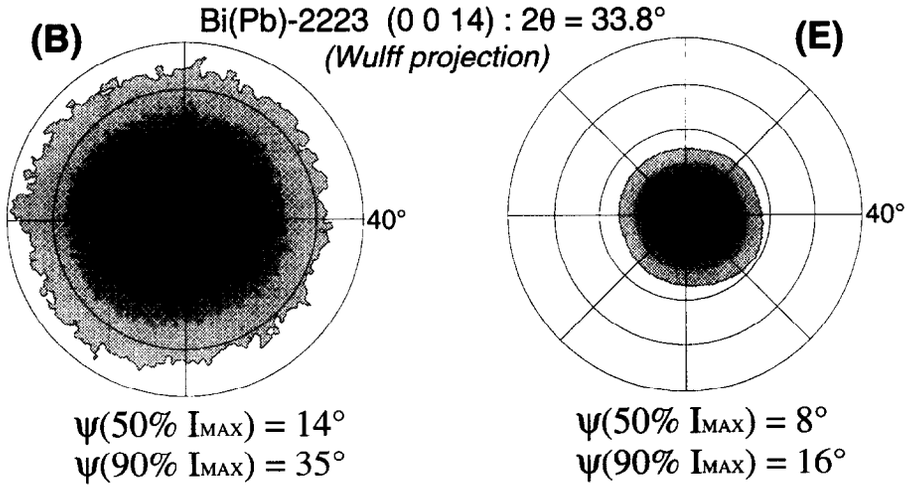

Fig. 2. (O O 14) pole figures performed on samples (B) and (E).

Table 1. Knoop hardness results

	A1	A2	A3	A	B	C	D	E
	Iso 1t	Iso 2t	Iso 3t	Isostatic	5 min/7MPa	5 min/20MPa	24h/15MPa	48h/15MPa
Density (%d_{th})	73·5	77·1	79	96 (simulate)	94	>96	>96	>96
Deformation (%)	—	—	—	—	54	~ 80	80	85
H_K ($\alpha = 90°$) (GPa)					2·3	2·7	2·5	3·2
H_K ($\alpha = 0°$) (GPa)	0·6	0·7	0·8	1·6	1·2	1	0·96	0·95
Mean H_K (GPa)					1·75	1·85	1·73	2·08
H_K (90°) - H_K (0°)				0	1·1	1·7	1·5	2·2

size, which slowly increases with time during the sinter-forging step, from 10 μm to 20 μm after 48 h. With a similar final thickness, the grain size is much higher in sample (E) and the number of grain boundaries is smaller. The hardness along the *c*-axis is thus ruled by the best links in a longer sinter-forging process.

(3) Apart from sample (E), the mean value of the hardness, which nearly corresponds to the one when the indent is oriented 45° with respect to the stress axis, is consistent with the calculated value obtained by a linear fit from the three cold isostatic-pressed and sintered samples (A_1) (A_2) and (A_3) : 1·6–1·8 GPa.

(4) The Knoop hardness in a direction normal to the stress axis remains relatively constant with the squash of the pellet, mainly controlled by the two parameters stress and time of the sinter-forging process, whereas along the stress axis, the hardness seems to depend more on the load than on the time of sinter-forging. The hardness of sample (C) is higher than that of, sample (D), due to the high stress (20 MPa), even if the loading time is much shorter. This shows that the short-time

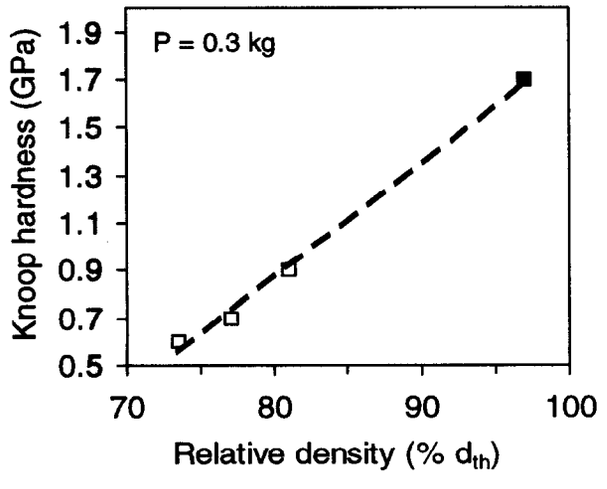

Fig. 3. Estimated Knoop hardness of a dense simulated isotropic 2223 ceramic.

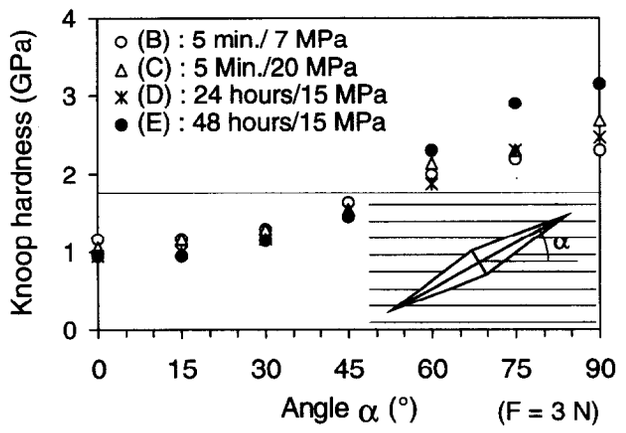

Fig. 4. Knoop hardness of samples (B) to (E) on polished cross sections vs angle α between the main impress axis and the mean texture orientation.

Table 2. Mechanical properties measured using three point bending loading

	B	B_A	C	C_A	D	D_A	E	E_A
	7 MPa/5 min		20 MPa/5 min		15 MPa/24 h		15 MPa/48 h	
σ_R(MPa)	130	110	180	150	160	140	200	170
K_{IC} (MPa$\sqrt{m}$)	1·8	1·8	2·1	2·1	2·7	2·5	2·8	2·9
E_{ab} (GPa)	91	86	105	86	91	90	120	120

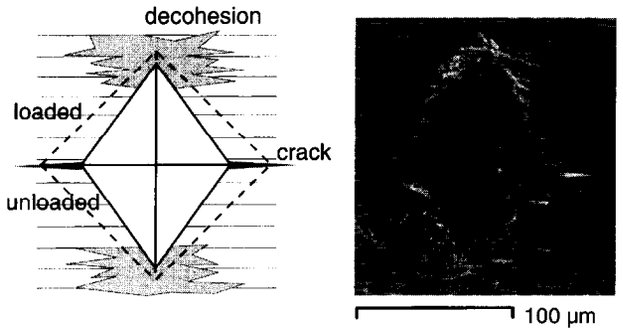

Fig. 5. Effect of the anisotropic microstructure on a Vickers indent performed on a polished and chemically revealed cross-section.

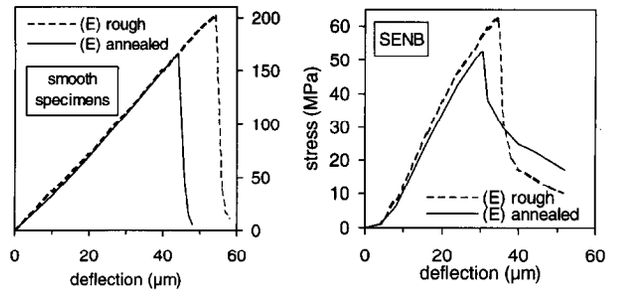

Fig. 6. Effect of the texture on the 3 point bending loading diagram of rough/annealed smooth and SENB (E) specimen, in flat-wise orientation.

sinter-forging under 20 MPa induces internal mechanical constraints that ameliorate the material. But in terms of superconductive properties, sample (C) exhibits a maximum transport critical current density J_{CT} of 3000 A/cm^2 at 77K without external magnetic field against 8000 A/cm^2 for sample (E). We have shown in a previous paper[11] that longer periods of the sinter-forging process are favourable for the 2223 superconductive ceramic to transport higher current densities.

3.2 Fracture

To allow the fracture results to be comparable, all the tested bars from the different batches were equally dimensioned and the initial relative flaw was a_0/w ~0·3, which corresponds to a_0 ~600 μm. Such a value is much larger than the grain size (0·2–0·5 μm) along w dimension. The 3-point bending tests on rough bars and air-annealed ones (B_A to E_A) are summarised in Table 2.

(1) Strength values of dense Bi-2223 vary in the range 100–200 MPa, depending on the texture quality. The post-annealing, useful to let the material recover good superconductive properties does not change the structural composition of the 2223 grains but does change their oxygen content and lowers the amount of secondary phases. That weakens the strength values by a constant factor of about 1·2 whatever the texture quality for samples (B) to (E).

(2) Elastic modulus is not affected after the annealing treatment excepted for the disc (C), which was too fast and barely sinter-forged.

These two observations reveal the presence of residual stresses due to the synthesis process. They seem to be less important in a few textured samples (B) or in slow hot-forged ones (D and E). In specimen (C), the relaxation of high internal residual stresses along the *c*-axis, due to annealing, favours the interlaminar shear in the plane (*ab*) which contributes to lowering the measured Young's modulus E_{ab}.

Regarding the fracture toughness values K_{IC}, the annealing treatment does not affect the resistance of the ceramic to the spreading of a major flaw. The load-deflection curves (Fig. 6), where the flaw spreads slower in annealed specimens than in rough ones, demonstrate this characteristic. The latter can be explained by an SEM observation of the fracture propagation. The good mutual align-

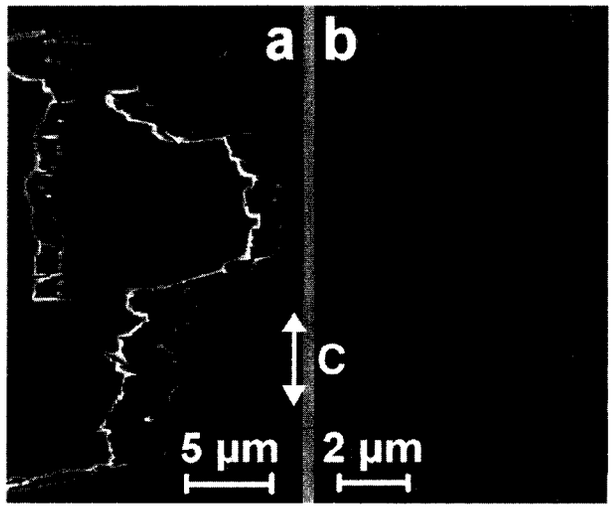

Fig. 7. (a) Details of the fracture profile with bridging effect of the grains, (b) slight influence of secondary phases on the crack path.

ment of the grains and the weak bonding between Bi-O layers in BSCCO superconductors, encourage the fracture to propagate itself in direction (*a–b*). In addition there is strong bridge effect between the decohesived grains due to their aspect ratios (Fig. 7 (a)). The secondary and non-superconductive phases, which represent an amount of 5 vol.% before the post-annealing and less than 3% after it, probably influence the mechanical properties but in a minor way according to the fracture toughness values. They do not seem to affect the crack propagation path, as can be seen by SEM observations (Fig. 7 (b)) that show the crack can deliminate the secondary grain or go through.

4 Conclusion

Hardness, strength and fracture toughness have been measured on textured $(Bi,Pb)_2Sr_2Ca_2Cu_3O_y$ superconductive ceramics. The study shows the importance of the sinter-forging processes regarding the mechanical properties. From poorly to highly textured samples and from rapid to slow/longer hot-forging treatments the Knoop hardness varies in the range 1·5–3·5 GPa along the sinter-forging axis, the strength in the range 100–200 MPa and the fracture toughness from 1·7 to 3 MPa$\sqrt{m}$ as measured in bulk specimens in the flat-wise orientation. This information is practical for the technological application of massive and highly textured sinter-forged Bi-2223 ceramics.

References

1. Chu, C.-Y., Routbort, J. L., Chen, N., Biondo, A. C., Kupperman, D. S. and Goretta, K. C., *Supercond. Sci. Technol*, 1992, **5**, 306–312.
2. Goretta, K. C., Loomans, M. E., Joo, J., Poeppel, R. B. and Chen, N., *Supercond. Sci. Technol.*, 1993, **6**, 282–286.
3. Chang, F., Ford, P. J., Saunders, G. A., Jiaqiang, L., Almond, D. P., Chapman, B., Cankurtaran, M., Poeppel, R. B. and Goretta, K. C., *Supercond. Sci. Technol.*, 1993, **6**, 484–489.
4. Ravinder, R., Reddy, M., Muralidhar, V., Hari Babu and Venugopal Reddy, P., *Supercond. Sci. Technol.*, 1995, **8**, 101–107.
5. Gao, W. and Vander Sande, J. B., *Supercond. Sci. Technol.*, 1992, **5**, 318–326.
6. Parnell, J. A., Dorris, S. E. and Larbalestier, D. C., *Phys. C*, 1994, **231**, 137–146.
7. Gherardi, L., Borgini, M., Caracino, P. and Metra, P., *Effect of mechanical stress and strain on the transport properties of BSCCO wires and tapes*, presented at the SATT5 Conference, 11–13 May, 1992, Capri, Italy.
8. Muralidhar, M., Nanda Kishore, K., Ramana, Y. V. and Hari Babu, V., *Mat. Sci. Eng.*, 1992, **B13**, 215–219.
9. Yuan, Y. S., Wong, M. S. and Wang, S. S., *J. Mater. Res.*, 1996, **31**, 1645–1652.
10. Luo, J., Stevens, R., Lo, W. and Campbell, A. M. *J. Mater. Sci.*, 1995, **30**, 3050–3056.
11. Rouessac, V., Wang, J., Provost, J. and Desgardin, G. *Phys. C*, 1996, **268**, 225–232.
12. Rouessac, V., Wang, J., Provost, J. and Desgardin, G. *J. Mater. Sci.*, 1996, **31**, 3387–3390.
13. Argyriou, D. N. and Vance, E. R. *J. Am. Ceram. Soc.*, 1992, **75**, 1269–1271.